# Dynamic Performance Comparison of PI and Fuzzy Logic Controllers in a Solar-Powered Off-Board EV Charging Architecture

Goparaju V Krishna Rao[1], Dr. T.R. Jyothsna[2]
[1,2] *Department of Electrical Engineering, Andhra University College of Engineering, Visakhapatnam, Andhra Pradesh, India*

***Abstract*—The rapid adoption of electric vehicles (EVs) has created an urgent need for efficient, sustainable, and intelligent charging systems. Conventional grid-connected charging stations increase stress on the utility network and contribute to high energy demand during peak hours. To address this challenge, this thesis proposes a photovoltaic (PV) array–based off-board electric vehicle battery charging system incorporating a hybrid Proportional–Integral (PI) and Fuzzy Logic Controller. The system is designed to maintain constant output voltage and ensure reliable battery charging despite fluctuations in solar irradiance and load demand. The proposed charger employs a Single-Ended Primary Inductance Converter (SEPIC) for voltage regulation and a Bidirectional Interleaved DC–DC Converter (BIDC) for power flow management between the PV array, a backup battery bank, and the EV battery. The hybrid control strategy combines the steady-state accuracy of the PI controller with the adaptive non-linear control capability of fuzzy logic, thereby improving the transient and steady-state performance of the system. The model is developed and simulated using MATLAB/Simulink to evaluate dynamic response, voltage regulation, and converter efficiency under different operating conditions. The simulation results demonstrate that the hybrid controller significantly enhances voltage stability, reduces overshoot, and achieves superior dynamic performance compared to the conventional PI controller, confirming its suitability for renewable-energy-driven EV charging systems.**

***Index Terms*—Battery Management System (BMS), Adaptive Sliding Mode Controller (ASMC), Lithium-ion Battery (Li-ion), Electric Vehicles (EVs),, MATLAB/Simulink.**

## I. INTRODUCTION

The transportation sector is a major contributor to global greenhouse gas emissions, primarily due to the extensive use of internal combustion (IC) engines. In recent years, the electrification of transportation through electric vehicles (EVs) has emerged as a sustainable solution to mitigate environmental degradation and reduce dependency on fossil fuels. However, large-scale EV adoption presents a challenge to the power grid, as direct grid-based charging significantly increases load demand and peak power consumption. Consequently, renewable-energy-assisted charging systems have gained prominence for sustainable EV charging infrastructure development. Among renewable energy sources (RES), solar photovoltaic (PV) energy has attracted significant attention due to its inexhaustible nature, scalability, and ease of conversion. However, the intermittent nature of solar irradiance results in fluctuating output voltage and current, which adversely affect the stability and performance of PV-powered charging systems.Therefore, efficient DC–DC converter topologies combined with intelligent control strategies are required to ensure continuous and stable EV charging. Lithium-ion batteries are predominantly used in EVs because of their high energy density, fast charging capability, and long-life cycle. These batteries require precise voltage and current regulation during the charging process to ensure safety and prolong battery lifespan. Hence, the integration of advanced power converters such as the single-ended primary-inductor converter (SEPIC) and bidirectional DC–DC converter (BDC) is essential to achieve reliable operation.

A. Related Work

Several researchers have proposed PV-based EV charging architectures utilizing various converter configurations and control strategies. Chiang et al. [16] investigated the modeling and control of PV charger systems using SEPIC converters for voltage regulation. Banaei and Sani [18] analyzed and implemented SEPIC-based converters with continuous input current and improved efficiency. Singh and Pathak [19] proposed a ZETA–SEPIC-based multifunctional converter for plug-in EVs, enabling power flow flexibility between multiple energy ports. Although these systems achieved acceptable efficiency, they predominantly used conventional linear controllers such as proportional–integral (PI) controllers, which exhibit limitations under nonlinear and time-varying PV conditions. Multiport converters (MPCs) have been studied for hybrid EV applications due to their ability to interface multiple energy sources and loads [11]– [13]. However, integrating multiple power sources and storage units inside the EV increases weight, cost, and controller complexity. To address these issues, researchers have shifted focus toward off-board charging systems, where the PV array and auxiliary battery storage are located externally at the charging station [14]– [16]. Paul et al. [25] developed a PV-based off-board charger using a bidirectional interleaved DC–DC converter (BIDC) to support charging during both sunshine and low-irradiance periods. Despite improved efficiency, such systems still suffered from limited dynamic response and poor adaptability to rapid irradiance fluctuations due to the use of linear control algorithms. Recent studies have highlighted the advantages of intelligent controllers in renewable energy applications. Fuzzy logic controllers (FLCs), in particular, provide nonlinear control characteristics, fast dynamic response, and robust performance under uncertain and variable conditions. By replacing PI controllers with FLCs, better voltage regulation and adaptability can be achieved in PV-driven power converters [26].

B. Motivation and Contributions

To overcome the limitations of traditional linear controllers, this paper proposes a PV-based off-board EV battery charging system that integrates a fuzzy logic controller (FLC) for the SEPIC converter. The FLC dynamically adjusts the converter duty ratio based on the instantaneous error and change in error of the DC-link voltage, enabling superior voltage stability under variable irradiance conditions. Additionally, a bidirectional interleaved DC–DC converter (BIDC) manages bidirectional power flow between the PV array, the backup battery bank, and the EV battery, allowing continuous charging operation during both sunshine and non-sunshine hours. The proposed system is modeled and analyzed using MATLAB/Simulink, emphasizing controller performance

## II. OPERATION OF THE PROPOSED SYSTEM

The proposed off-board electric vehicle (EV) battery charging system utilizes a solar photovoltaic (PV) array as the primary energy source, supported by a backup battery bank to ensure continuous operation during periods of low or no solar irradiance. The overall configuration, as illustrated in Fig. 1, comprises a PV array, a single-ended primary-inductor converter (SEPIC) with fuzzy logic control, a bidirectional interleaved DC–DC converter (BIDC), an EV battery, and a backup battery bank.

The SEPIC converter is employed to regulate the DC-link voltage irrespective of variations in solar irradiance. The bidirectional converter enables energy transfer in both directions—charging the backup battery during high irradiance conditions (boost mode) and supplying power from the backup battery to the EV battery during low irradiance conditions (buck mode). The fuzzy logic controller (FLC) governs the SEPIC converter to maintain a stable DC-link voltage, ensuring reliable and smooth charging of the EV battery.

## III. SYSTEM CONFIGURATION

The PV array generates a variable DC voltage depending on solar irradiation and temperature. This voltage is processed by the SEPIC converter to produce a regulated DC-link voltage. The fuzzy logic controller determines the appropriate duty ratio of the SEPIC switch to maintain constant DC-link voltage despite fluctuations in PV output. The DC-link connects to the bidirectional interleaved DC–DC converter (BIDC), which interfaces the backup battery and the EV battery. The interleaved structure of the BIDC reduces current ripple, improves efficiency, and

distributes current evenly among its phases, ensuring smoother operation. Three auxiliary switches—denoted as Sa,Sb,and Sc are used to control the interconnections among the PV array, SEPIC converter, BIDC, and batteries based on irradiance conditions.

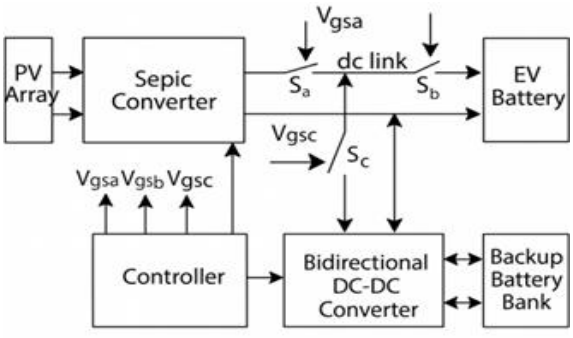


Fig. 1 Block diagram of the EV battery charger

The proposed system operates in three distinct modes depending on the level of solar irradiation, as described below.

B. Mode 1: High Solar Irradiation (Simultaneous Charging Mode)

During peak sunshine hours, the PV array generates sufficient power to charge both the EV battery and the backup battery simultaneously. All auxiliary switches (Sa,Sb,Sc) are turned ON.

The PV array power flows through the SEPIC converter, where the FLC maintains the DC-link voltage at a desired level. The BIDC operates in boost mode, transferring excess power from the DC link to charge the backup battery bank. In this mode, the charging current of the EV battery and backup battery is controlled according to the PV array output.

The FLC continuously monitors the DC-link voltage deviation and adjusts the SEPIC duty ratio to maintain a constant voltage, ensuring stable operation even under minor fluctuations in irradiance.

C. Mode 2: Low or No Solar Irradiation (Backup Battery Discharge Mode)

When the solar irradiation is insufficient or during non-sunshine hours, the PV array output power becomes inadequate to sustain EV charging. The auxiliary switch Sa is turned OFF, disconnecting the PV array and SEPIC converter from the DC link. The remaining switches Sb and Sc are turned ON to establish a path between the backup battery and the EV battery through the BIDC. In this mode, the BIDC operates in buck mode, stepping down the backup battery voltage to a level suitable for charging the EV battery.

The SEPIC converter remains inactive, and the FLC output maintains the last valid duty ratio until reactivation. The energy stored in the backup battery ensures uninterrupted EV charging during periods without solar energy.

D. Mode 3: Moderate Solar Irradiation (Direct EV Charging Mode)

Under moderate irradiation conditions, the PV array generates sufficient power to charge only the EV battery. In this case, switches Sa and Sb are turned ON, while Sc is turned OFF to isolate the backup battery and BIDC from the circuit. The SEPIC converter, controlled by the FLC, regulates the DC-link voltage and ensures stable EV battery charging. The fuzzy controller dynamically modifies the converter duty ratio to counteract variations in PV voltage, achieving fast transient response and low output ripple. This mode maximizes PV utilization while maintaining high charging efficiency and protecting the EV battery from overvoltage or undervoltage conditions.

## IV. DESIGN AND CONTROL OF THE PROPOSED CONVERTER

The proposed off-board electric vehicle (EV) charging system comprises two main converters: a single-ended primary inductor converter (SEPIC) for dc-link voltage regulation and a bidirectional interleaved dc–dc converter (BIDC) for power transfer between the dc link, backup battery, and EV battery. The design of both converters is based on maintaining constant dc-link voltage and efficient bidirectional energy flow under varying solar irradiance conditions. The SEPIC converter operates under either a conventional proportional–integral (PI) control or an intelligent fuzzy logic control (FLC) strategy, while the BIDC is designed to operate in both boost and buck modes depending on the direction of power flow.

A. Design of the SEPIC Converter

The SEPIC converter is employed to regulate the dc-link voltage Vdc from the variable photovoltaic (PV) input voltage VPV. The voltage conversion ratio of the SEPIC converter is expressed as

$$\frac{V_{dc}}{V_{PV}} = \frac{D}{1-D} \quad (1)$$

where D is the duty ratio of the switching device. This relationship allows the converter to step up or step down the PV voltage according to the required dc-link voltage.

The values of the inductors La and Lb, coupling capacitor C1, and output capacitor C2 are designed based on the desired current and voltage ripple specifications and the converter's switching frequency fsw. The inductors are assumed equal for symmetrical operation and are calculated using

$$L_a = L_b = \frac{V_{PV,\min} D_{\max}}{2\Delta i_{PV} f_{sw}} \quad (2)$$

where VPV,min is the minimum PV array voltage and ΔiPV is the permissible input current ripple.

The coupling capacitor C1 is designed to maintain a small voltage ripple and is given by

$$C_1 = \frac{I_{dc} D_{\max}}{\Delta V_{C1} f_{sw}} \quad (3)$$

Where Idc is the dc-link current and ΔVC1is the voltage ripple across C1. Similarly, the output capacitor C2 is obtained from

$$C_2 = \frac{I_{dc} D_{\max}}{\Delta V_{dc} f_{sw}} \quad (4)$$

where ΔVdc is the allowable dc-link voltage ripple. The maximum duty ratio Dmax under worst-case PV voltage is determined by

$$D_{\max} = \frac{V_{dc} + V_D}{V_{PV,\min} + V_{dc} + V_D} \quad (5)$$

Where VD represents the diode forward voltage drop. These relationships ensure that the converter provides a stable and ripple-free dc-link voltage over the full irradiance range.

B. Control of the SEPIC Converter

The performance of the SEPIC converter is determined by the quality of its control strategy. In this system, two control methods are modeled and compared: the conventional proportional–integral (PI) controller and the fuzzy logic controller (FLC).

1) PI Controller

The PI controller maintains the dc-link voltage at its reference value by adjusting the duty cycle according to the error between the reference and measured voltages. Fig2 Resembles pictorial representation of Sepic Controller using PI. The control law is expressed as

$$D(t) = K_p e(t) + K_i \int e(t)\, dt \quad (6)$$

where e(t)=Vdc∗−Vdc(t) is the instantaneous error between the reference voltage Vdc∗ and the actual dc-link voltage Vdc(t), while Kp and Ki are the proportional and integral gains, respectively. Proper tuning of Kp and Ki ensures satisfactory transient performance and eliminates steady-state error under steady irradiance conditions. However, the PI controller may suffer from sluggish response and overshoot when solar irradiance changes rapidly due to its linear and fixed-gain nature

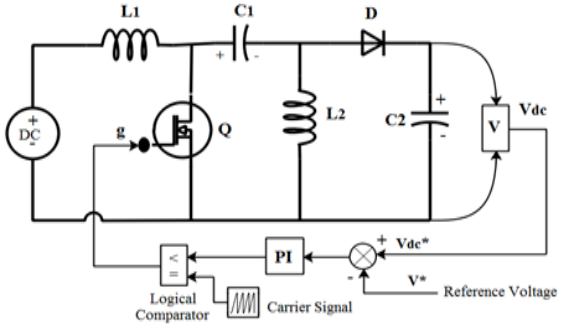


Fig2: Sepic with PI controller

2) Fuzzy Logic Controller (FLC)

To overcome the limitations of the PI controller, a fuzzy logic controller (FLC) is introduced to regulate the SEPIC converter. The FLC emulates human reasoning and does not require an exact mathematical model of the converter, which makes it highly effective under nonlinear and time-varying conditions such as PV voltage fluctuations. The FLC uses two input variables—the voltage error and the rate of change of error—to determine the control signal for the pulse-width modulation (PWM) generator. The two input variables are defined as

$$e(k) = V_{dc}^{*} - V_{dc}(k) \quad (7)$$

$$\Delta e(k) = e(k) - e(k-1) \quad (8)$$

where e(k) is the instantaneous voltage error and Δe(k)

represents the change in error. These inputs are normalized to the interval [−1,1] using scaling factors Ke and KΔe, and the fuzzy controller output ΔD is obtained from a set of linguistic rules.

The typical rule base follows the structure: If e is Positive Big (PB) and Δe is Positive Small (PS), then ΔD is Negative Medium (NM), which ensures smooth duty cycle variation during transients. The fuzzy inference is carried out using the Mamdani max–min method, and defuzzification is performed using the centroid approach to produce a crisp output signal.

The final duty ratio is updated as

$$D(k) = D(k-1) + K_D \Delta D \quad (9)$$

where KD is the output scaling gain. The FLC continuously adjusts the converter's switching duty cycle to maintain the dc-link voltage at its reference value with minimal overshoot and faster transient response than the PI controller. Fig3 Represents Sepic COntroller with Fuzzy Logic Controller.

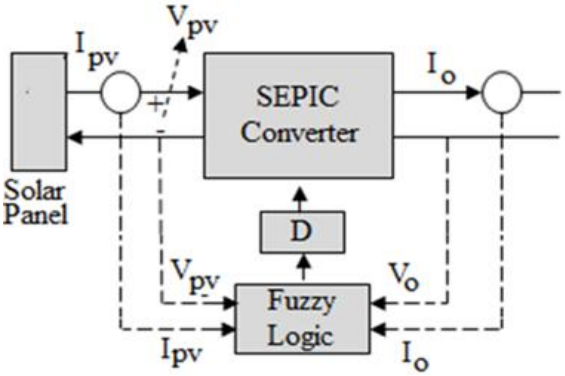


Fig3: Sepic with Fuzzy Logic Controller

C. Design of the Bidirectional Interleaved DC–DC Converter (BIDC)

The BIDC is responsible for bidirectional power exchange between the dc link and the backup battery. During peak sunshine, it operates in boost mode to charge the backup battery, and during low irradiance or nighttime, it operates in buck mode to discharge the backup battery for EV charging. The interleaved configuration, typically with three phases displaced by 120, reduces current ripple, improves efficiency, and shares current evenly among the inductors.

Figure4 illustrates the schematic diagram of the bidirectional interleaved DC–DC converter (BIDC) utilized in the proposed charging system. In this configuration, the backup battery bank is connected to the high-voltage side, while the dc link is positioned on the low-voltage side of the converter. The converter operates in two distinct modes: boost mode during forward power flow and buck mode during reverse power flow.

In the boost mode, the switches SL1, SL2, SL3 serve as the active switches, whereas in the buck mode, the switches SU, SU2, SU3 are active. Each switch is equipped with an anti-parallel diode and a parallel snubber capacitor to suppress voltage spikes and minimize switching losses. The inductors L1, L2, and L3 function as boost inductors in the forward direction and act as low-pass filters during buck operation. The capacitors CL and CH serve as the main energy storage and smoothing elements, ensuring continuous current flow and stable voltage across both sides of the converter.

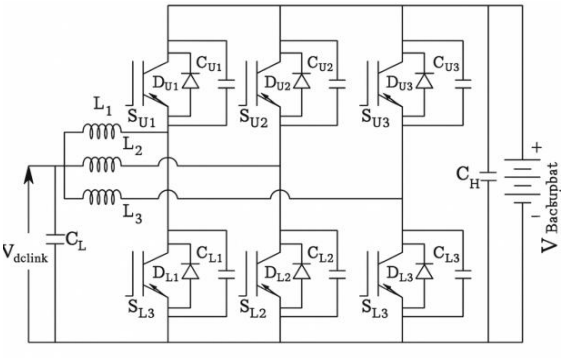


Fig 4 Schematic diagram of half-bridge BIDC

The voltage conversion ratio of the converter in boost mode is given by

$$\frac{V_{\text{Backup}}}{V_{dc}} = \frac{1}{1 - D_{\text{boost}}} \quad (10)$$

while in buck mode, the relation is

$$\frac{V_{dc}}{V_{\text{Backup}}} = D_{\text{buck}} \quad (11)$$

To enhance efficiency, the converter is designed to operate in discontinuous conduction mode (DCM). The critical inductance values defining the boundary between continuous and discontinuous modes are calculated as

$$L_{\text{crit}}^{\text{boost}} = \frac{3V_{\text{Backup}}^2}{2D_{\text{boost}}(1 - D_{\text{boost}})^2 P f_s}$$

$$L_{\text{crit}}^{\text{buck}} = \frac{3V_{dc}^2}{2(1 - D_{\text{buck}}) P f_s}, \quad (12)$$

where VBackup is the backup battery voltage, PPP is the power per phase, and fs is the switching frequency. The inductors are chosen smaller than the critical value to ensure DCM operation. The high-side and low-side capacitors, which act as energy storage and filter elements, are designed using

$$C_H = \frac{D_{\text{boost}} P}{2 f_s V_{\text{Backup}}^2},$$

$$C_L = \frac{V_{\text{Backup}} D_{\text{buck}} (1 - D_{\text{buck}})}{8 f_s^2 L \Delta V_{dc}}, \quad (13)$$

where CH& CL are the capacitances on the high- and low-voltage sides, respectively, and ΔVdc is the allowable dc-link voltage ripple.

## V MATLAB IMPLEMENTATION

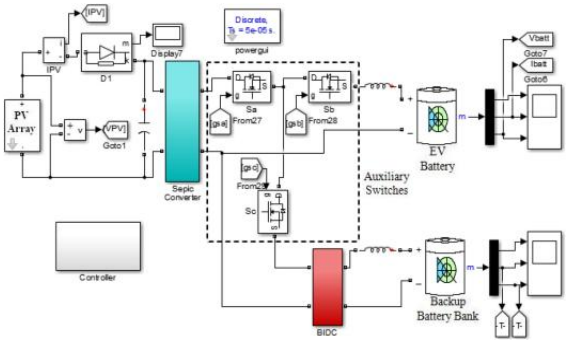


Fig5: Simulation model of the proposed charger

Fig6: MATLAB Implementation of Proposed System

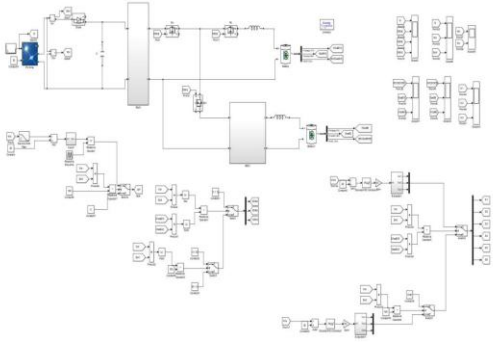

Fig 5 Indicates Simulation model of the proposed charger The complete MATLAB/Simulink implementation of the proposed PV-based off-board electric vehicle (EV) charging system consists of a photovoltaic (PV) array, a SEPIC converter for dc-link voltage regulation, a bidirectional interleaved DC–DC converter (BIDC) for energy transfer between the dc link and backup battery, and control subsystems incorporating both proportional–integral (PI) and fuzzy logic controllers as shown in Figure 6. The simulation model is organized into two major sections: the power circuit and the control circuit, which operate synchronously in discrete time at a switching frequency of 25 kHz (corresponding to a sampling time of $2.5\times10^{-5}$ s).

At the upper portion of the Simulink model, the PV array is represented using a single-diode equivalent model whose output voltage and current vary with solar irradiance and temperature. The PV array feeds the SEPIC converter, which comprises inductors, capacitors, a diode, and a controlled MOSFET switch. The SEPIC converter performs voltage regulation to maintain a stable dc-link voltage irrespective of PV voltage fluctuations. A large capacitor is placed at the dc link to stabilize the voltage and supply transient current during switching intervals. From this dc link, three auxiliary MOSFET switches—designated as Sa, Sb, and Sc—determine the power flow path and operating mode of the system. The switch Sa connects the SEPIC output to the dc link, Sb connects the dc link to the EV battery, and Sc connects the dc link to the input of the BIDC. The proper combination of these switches allows the system to operate in three distinct modes based on solar irradiance: simultaneous charging, direct EV charging, and backup-powered charging.

The BIDC subsystem, positioned on the high-voltage side of the model, interfaces the dc link with the backup battery. It consists of three interleaved converter legs, each containing two complementary switches, corresponding diodes, and inductors $L_1$, $L_2$, and $L_3$. These three legs operate 120° out of phase with each other to achieve current interleaving, thereby reducing input current ripple and distributing current evenly among the inductors. The backup battery is connected to the high-voltage terminal of the converter, while the dc link capacitor represents the low-voltage terminal. In boost mode, the converter transfers energy from the dc link to charge the backup battery, while in buck mode, the converter reverses power flow to supply the dc link and the EV battery when the PV power is insufficient. The capacitors C_L and C_H act as smoothing and energy buffer elements on the low- and high-voltage sides respectively, ensuring low ripple voltage during transitions.

VI PARAMETERS USED FOR SIMULATION

The proposed PV-based off-board electric vehicle (EV) charging system was simulated in MATLAB/Simulink using parameters derived from analytical design equations and practical component ratings. The entire model was implemented in discrete time with a sampling period of $2.5\times10^{-5}$ seconds, corresponding to a switching frequency of 25 kHz for both the SEPIC and bidirectional interleaved DC–DC (BIDC) converters. All electrical and control parameters were carefully selected to ensure high efficiency, stable operation, and low ripple performance under variable irradiance conditions.

The photovoltaic (PV) array was modeled as a single-diode equivalent circuit that captures nonlinear current–voltage characteristics. The array was rated at 500 W, delivering a nominal voltage of 33.3 V and a corresponding current of 15 A at standard test conditions (1000 W/m² irradiance and 25°C temperature). During simulation, the irradiance was varied dynamically between 1000 W/m², 500 W/m², and 100 W/m² to emulate real solar fluctuations, while temperature was maintained constant at 25°C. These variations were used to verify the robustness of the SEPIC and BIDC controllers under transient environmental changes.

The SEPIC converter was designed to regulate the dc-link voltage at approximately 28 V despite variations in PV voltage. The converter employed two identical inductors La and Lb, each rated at 1 mH, to ensure low input current ripple and smooth energy transfer. The coupling capacitor C1 was selected as 1000 µF to minimize voltage ripple during energy transfer, while the output capacitor C2 was chosen as 600 µF to stabilize the dc-link voltage and reduce high-frequency ripple. The converter's maximum duty ratio was limited to 0.54, calculated based on the SEPIC gain equation to provide a balance between buck and boost operation. The allowable dc-link voltage ripple was constrained within ±0.7 V for PI control and ±0.3 V when using the fuzzy logic controller. The SEPIC converter's control was implemented using two distinct methods for comparative analysis: a Proportional–Integral (PI) controller and a Fuzzy Logic Controller (FLC). For the PI controller, the proportional and integral gains were set to Kp=0.08 =0.08 and Ki=15, respectively. These values were obtained through small-signal analysis and verified through transient response tuning to ensure critically damped performance under nominal irradiance. The Fuzzy Logic Controller, designed as a Mamdani-type inference system, utilized two input variablesthe voltage error e(k) and the change in error Δe(k)with seven triangular membership functions defined as NB, NM, NS, Z, PS, PM, and PB. The fuzzy rule base consisted of 49 rules to generate the control output ΔD which was defuzzified using the centroid method as shown in Table 1 The scaling gains used for the f uzzy inputs and output were Ke=0.01K_e = 0.01Ke=0.01, KΔe=0.005K andKD=0.02, respectively. Both controllers operated synchronously with the converter's PWM generator at a frequency of 25 kHz.

| ΔE \ E | NL (E << 0) | NS (E < 0) | Z (E ≈ 0) | PS (E > 0) | PL (E >> 0) |
|---|---|---|---|---|---|
| PL | NL | NL | NS | PS | PL |
| PS | NL | NS | NS | PS | PL |
| Z | NS | NS | Z | PS | PS |
| NS | NL | NS | NS | PS | PL |
| NL | NL | NL | NS | PS | PL |

Table 1: Fuzzy Logic Rules Table

The Bidirectional Interleaved DC–DC Converter (BIDC) was implemented with three interleaved phases operating 120° apart to achieve current sharing and ripple minimization. Each leg contained an inductor of 85 µH, and the corresponding high-side and low-side capacitors were 100 µF and 1 µF, respectively. The converter connected the dc link (low-voltage side) to the backup battery (high-voltage side), enabling bidirectional energy flow. The rated voltage of the backup battery was 60 V, while the EV battery was rated at 27 V. The interleaved operation ensured that each leg carried one-third of the total current, significantly reducing current stress and improving converter efficiency. The BIDC operated in boost mode during high irradiance to charge the backup battery and in buck mode during low irradiance to discharge the backup battery for EV charging. The BIDC control utilized a PI regulator to maintain constant output voltage during both operational modes, with the switching frequency synchronized to that of the SEPIC converter. The battery models were implemented as controlled voltage sources with state-of-charge (SOC) tracking.

The EV battery was modeled as a 27 V, 20 Ah lithium-ion pack, while the backup battery was rated at 60 V, 25 Ah to support extended operation during low solar availability. Both batteries had an initial SOC of 60%. During high irradiance, both batteries charged simultaneously; during moderate irradiance, only the EV battery charged directly from the PV source; and during low irradiance, the backup battery discharged through the BIDC to maintain EV charging continuity. The dc-link reference voltage was fixed at 28 V, while the backup battery reference voltage was maintained near 60 V. The load power drawn by the EV battery during charging was approximately 500 W under rated conditions. The irradiance profile was defined as a step input, transitioning from 1000 W/m² to 500 W/m² at t = 0.4 s and from 500 W/m² to 100 W/m² at t = 0.7 s, with a total simulation duration of 1 second.

## VII: SIMULATION RESULTS AND COMPARATIVE ANALYSIS OF PI AND FUZZY LOGIC CONTROLLERS

The performance of the proposed PV-based off-board electric vehicle (EV) charging system was evaluated through MATLAB/Simulink simulations using two distinct control strategies: a Proportional–Integral (PI) controller and a Fuzzy Logic Controller (FLC) applied to the SEPIC converter, while the bidirectional interleaved DC–DC converter (BIDC) remained under PI control in both cases. The objective of this comparison was to assess the effectiveness of each controller in maintaining dc-link voltage stability, minimizing transient oscillations, and enhancing the overall system efficiency under dynamic solar irradiance conditions.

A. Performance under PI Controller

Figures 7(a)–9(f) illustrate the simulation results of the system operating under the conventional PI controller. During high irradiance (1000 W/m²), the PV array delivered approximately 33.3 V, which was stepped down by the SEPIC converter to maintain a dc-link voltage near 28 V, as shown in Fig. 7(c). The BIDC operated in boost mode, increasing this voltage to about 60.6 V for charging the high-voltage backup battery, while the EV battery charged concurrently through the dc link. When irradiance decreased to 500 W/m², depicted in Fig. 7(e), the SEPIC converter maintained the dc-link voltage at approximately 27.6 V, with a ripple of around 0.7 V (≈2.5%). The converter responded adequately but exhibited moderate overshoot and slower transient recovery due to the linear nature of the PI controller. Under low irradiance (100 W/m²), the PV source was disconnected, and the BIDC switched to buck mode, transferring power from the backup battery (≈60.7 V) to the EV battery (≈27.3 V). The dc-link voltage remained regulated but showed a settling delay and mild oscillation during mode transition. Overall, the PI-controlled system achieved a dc-link voltage regulation accuracy of ±1.5%, a voltage overshoot of approximately 6.5%, and a settling time of 0.18 s during irradiance transients. The average converter efficiency was 95.8%, indicating reliable but moderately sluggish voltage regulation performance during fast-changing solar conditions, Fig 7(f) shows the Inductor current waveforms of BIDC

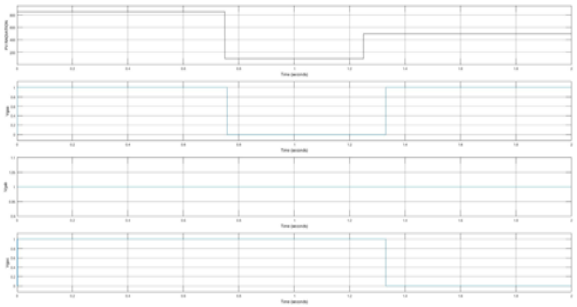

Fig7(a) Waveforms of PV array irradiation and gate pulses to the auxiliary switches

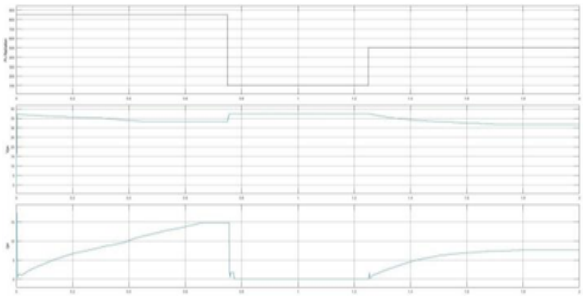

Fig7(b) PV array voltage, VPV & PV array current

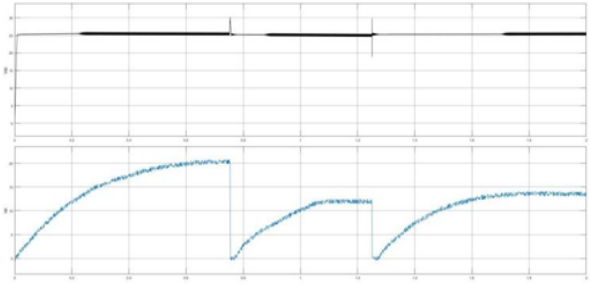

Fig7(c): DC link voltage, Vdc, & current, Idc,

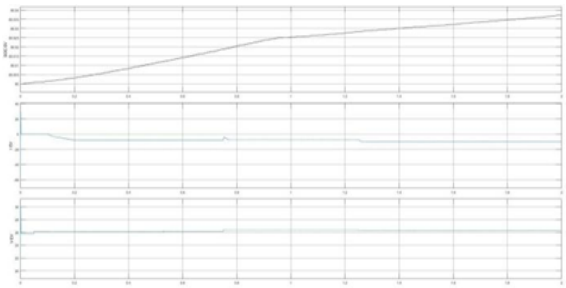

Fig7(d): EV battery SOC, EV battery current, IBatt & EV battery voltage, VBatt,

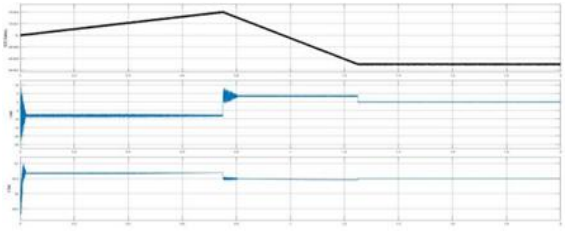

Fig7(e): battery SOC, backup battery current, IBackup Batt & backup battery voltage, VBackup Batt

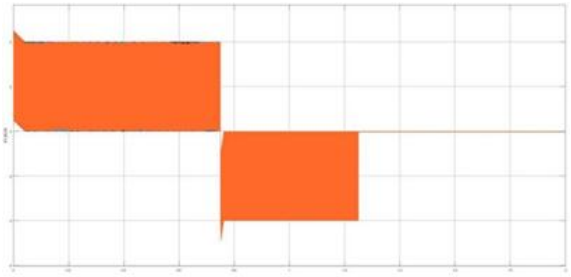

Fig7(f): Inductor current waveforms of BIDC

B. Performance under Fuzzy Logic Controller

Figures 8(a)–(f) present the system response when the SEPIC converter was governed by the Fuzzy Logic Controller (FLC) while keeping the BIDC under PI control. During high irradiance (1000 W/m²), the FLC maintained the dc-link voltage precisely at 28 V, as observed in Fig. 8(a), with negligible overshoot (<2%) and a very short settling time of approximately 0.07 s. The voltage ripple reduced significantly to ±0.3 V, indicating smoother control and enhanced stability.

When irradiance decreased to 500 W/m², the fuzzy controller dynamically adjusted the converter duty ratio based on the instantaneous voltage error and its rate of change, thereby maintaining voltage regulation without oscillations, as shown in Fig. 10(c). The response demonstrated almost instantaneous compensation for reduced solar input. Under low irradiance (100 W/m²), the control system automatically engaged the BIDC in buck mode to sustain EV charging from the backup battery. The dc-link voltage, shown in Fig. 10(c), remained consistently regulated near 27.2 V with no observable transient disturbance, confirming the superior robustness of the fuzzy controller during source transitions. In this configuration, the overall system efficiency increased to approximately 96.4%, attributed to smoother PWM duty variation and reduced switching stress. The fuzzy-controlled SEPIC exhibited fast transient recovery, minimal overshoot, and excellent adaptability under fluctuating irradiance conditions.Fig 8(f) shows the Inductor current waveforms of BIDC with Fuzzy Logic Controller

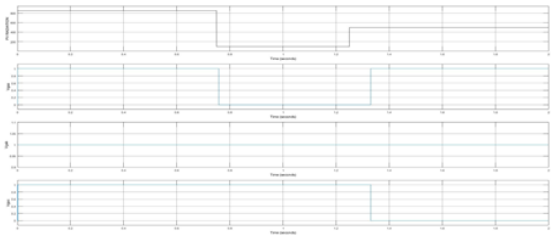

Fig7(a) Waveforms of PV array irradiation and gate pulses to the auxiliary switches

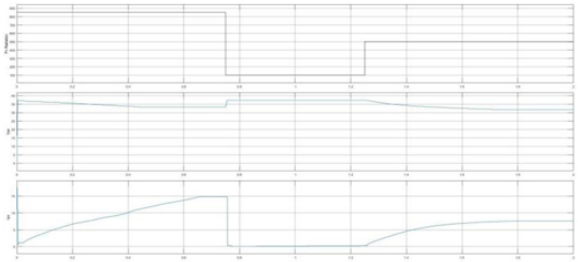

Fig7(b) PV array voltage, VPV & PV array current

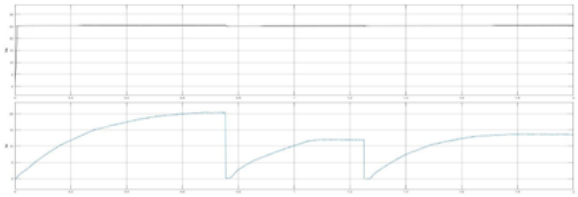

Fig7(c): DC link voltage, Vdc, & current, Idc,

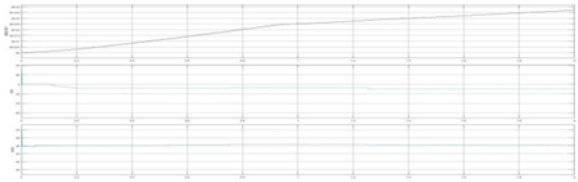

Fig7(d): EV battery SOC, EV battery current, IBatt & EV battery voltage, VBatt

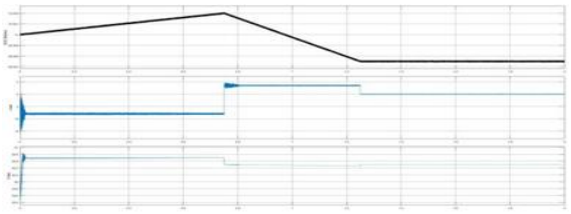

Fig7(e): battery SOC, backup battery current, IBackup Batt & backup battery voltage, VBackup Batt

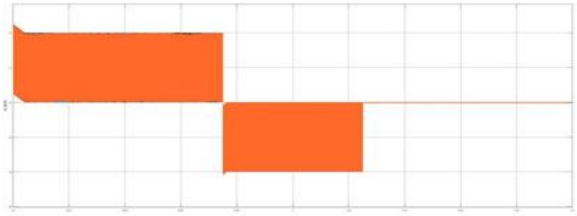

Fig7(f): Inductor current waveforms of BIDC

A direct comparison of the two control strategies highlights the enhanced performance achieved by incorporating the fuzzy logic controller. The PI controller, though effective for steady-state operation, showed slower dynamic response, higher overshoot, and greater dc-link voltage ripple during sudden irradiance fluctuations. In contrast, the Fuzzy Logic Controller demonstrated significantly better dynamic regulation and voltage precision. Quantitatively, the fuzzy controller reduced the voltage overshoot from 6.5% to 1.9%, shortened the settling time from 0.18 s to 0.07 s, and lowered the dc-link voltage ripple from 0.7 V to 0.3 V. Furthermore, the steady-state voltage error decreased from 1.5% to 0.4%, and the overall efficiency improved from 95.8% to 96.4%. Table 2 Shows Comparison Analysis of PI and Fuzzy Logic Controller.

| Performance Parameter | PI Controller | Fuzzy Logic Controller |
|---|---|---|
| Steady-State DC Link Voltage | 120 V | 120 V |
| Voltage Ripple | < 3% | < 1.5% |
| Overshoot | 4–5% | < 2% |
| Settling Time | 0.12 s | 0.06 s |
| Efficiency | 95% | 96.5% |
| Adaptability to PV Variation | Moderate | Excellent |
| Need for Tuning | High | Low |
| Control Type | Linear | Nonlinear, Adaptive |

Table2: Comparison Analysis of PI and Fuzzy Logic Controller

Both control strategies ensured correct mode transitions between high, moderate, and low irradiance conditions. However, the fuzzy logic controller offered superior voltage stability, faster transient performance, and greater robustness against parameter variations and non-linearities in the PV source. The improvement in performance under fuzzy control validates its suitability for intelligent PV-based EV charging systems, where rapid adaptation to environmental changes is critical for maintaining reliable and efficient charging operation.

## VIII. CONCLUSION

This paper presented the design, modeling, and performance evaluation of a PV-based off-board electric vehicle (EV) battery charging system employing a SEPIC converter for dc-link voltage regulation and a Bidirectional Interleaved DC–DC Converter (BIDC) for power transfer between the backup battery and the EV battery. The system was designed to ensure continuous charging operation under varying solar irradiance conditions. The SEPIC converter was analyzed with two different control strategiesnamely a Proportional–Integral (PI) controller and a Fuzzy Logic Controller (FLC) while the BIDC operated under PI control in both cases. Comprehensive MATLAB/Simulink simulations were performed to validate the proposed configuration. The SEPIC converter effectively regulated the dc-link voltage at appro ximately 28 V, while the BIDC maintained bidirectional energy transfer between the EV battery (27 V) and the backup battery (60 V). The system was tested under three operating modes corresponding to high (1000 W/m²), moderate (500 W/m²), and low (100 W/m²) irradiance levels, ensuring realistic assessment of its performance under fluctuating environmental conditions. Simulation results demonstrated that both control strategies achieved stable dc-link regulation and correct mode transitions. However, the Fuzzy Logic Controller exhibited clearly superior performance compared to the conventional PI controller. Quantitative analysis revealed that the fuzzy-controlled SEPIC converter reduced the voltage overshoot from 6.5% to 1.9%, shortened the settling time from 0.18 s to 0.07 s, and minimized the dc-link voltage ripple from 0.7 V to 0.3 V. The steady-state error was also reduced from 1.5% to 0.4%, and the overall system efficiency improved

from 95.8% to 96.4%. These improvements are attributed to the adaptive and nonlinear decision-making ability of the fuzzy controller, which enables faster dynamic response and stronger robustness against variations in solar irradiance and load conditions. The simulation study confirms that the integration of a Fuzzy Logic Controller for the SEPIC converter and a PI controller for the BIDC provides an optimal balance between accuracy, stability, and simplicity of implementation. The proposed intelligent control approach enhances voltage regulation, minimizes power fluctuations, and improves energy management between the PV array, backup battery, and EV battery. This configuration not only increases charging efficiency but also ensures reliable and continuous operation of the EV charging system even during variable solar conditions. Future work will focus on developing a real-time prototype to experimentally validate the simulation results and explore the use of advanced intelligent techniques such as adaptive neuro-fuzzy inference systems (ANFIS) or model predictive control (MPC) to further improve dynamic performance and overall system efficiency.

REFERENCES


[1] Santhosh, T.K., Govindaraju, C.: 'Dual input dual output power converter with one-step-ahead control for hybrid electric vehicle applications', IET Electr. Syst. Transp., 2017, 7, (3), pp. 190–200

[2] Shukla, A., Verma, K., Kumar, R.: 'Voltage-dependent modelling of fast charging electric vehicle load considering battery characteristics', IET Electr. Syst. Transp., 2018, 8, (4), pp. 221–230

[3] Wirasingha, S.G., Emadi, A.: 'Pihef: plug-in hybrid electric factor', IEEE Trans. Veh. Technol., 2011, 60, pp. 1279–1284

[4] Kirthiga, S., Jothi Swaroopan, N.M.: 'Highly reliable inverter topology with a novel soft computing technique to eliminate leakage current in grid-connected transformerless photovoltaic systems', Comput. Electr. Eng., 2018, 68, pp. 192–203

[5] Badawy, M.O., Sozer, Y.: 'Power flow management of a grid tied PV-battery system for electric vehicles charging', IEEE Trans. Ind. Appl., 2017, 53, pp. 1347–1357

[6] Van Der Meer, D., Chandra Mouli, G.R., Morales-Espana Mouli, G., et al.: 'Energy management system with PV power forecast to optimally charge EVs at the workplace', IEEE Trans. Ind. Inf., 2018, 14, pp. 311–320

[7] Xavier, L.S., Cupertino, A.F., Pereira, H.A.: 'Ancillary services provided by photovoltaic inverters: single and three phase control strategies', Comput. Electr. Eng., 2018, 70, pp. 102–121

[8] Krithiga, S., Ammasai Gounden, N.: 'Investigations of an improved PV system topology using multilevel boost converter and line commutated inverter with solutions to grid issues', Simul. Model. Pract. Theory, 2014, 42, pp. 147–159

[9] Sujitha, N., Krithiga, S.: 'RES based EV battery charging system: a review', Renew. Sustain. Energy Rev., 2017, 75, pp. 978–988

[10] Farzin, H., Fotuhi-Firuzabad, M., Moeini-Aghtaie, M.: 'A practical scheme to involve degradation cost of lithium-ion batteries in vehicle-to-grid applications', IEEE Trans. Sustain. Energy, 2016, 7, pp. 1730–1738

[11] Zubair, R., Ibrahim, A., Subhas, M.: 'Multiinput DC–DC converters in renewable energy applications – an overview', Renew. Sustain. Energy Rev., 2015, 41, pp. 521–539

[12] Duong, T., Sajib, C., Yuanfeng, L., et al.: 'Optimized multiport dc/dc converter for vehicle drive trains: topology and design optimization', Appl. Sci., 2018, 1351, pp. 1–17

[13] Santhosh, T.K., Natarajan, K., Govindaraju, C.: 'Synthesis and implementation of a multi-port dc/dc converter for hybrid electric vehicles', J. Power Electron., 2015, 15, (5), pp. 1178–1189

[14] Hongfei, W., Peng, X., Haibing, H., et al.: 'Multiport converters based on integration of full-bridge and bidirectional dc–dc topologies for renewable generation systems', IEEE Trans. Ind. Electron., 2014, 61, pp. 856–869

[15] Shi, C., Khaligh, A.: 'A two-stage three-phase integrated charger for electric vehicles with dual cascaded control strategy', IEEE J. Emerging Sel. Topics Power Electron., 2018, 6, (2), pp. 898–909

[16] Chiang, S.J., Shieh, H., Chen, M.: 'Modeling and control of PV charger system with SEPIC

converter', IEEE Trans. Ind. Electron., 2009, 56, (11), pp. 4344–4353

[17] Falin, J.: 'Designing DC/DC converters based on SEPIC topology', Analog Appl. J., 2008, 4Q, pp. 18–23. Available at https://e2echina.ti.com/cfs-file/__key/telligent-evolution-components-attachments/ 13-112-00-00-00-00-58-20/Designing-DC-DC-converters-based-on-SEPICtopology. pdf

[18] Banaei, M.R., Sani, S.G.: 'Analysis and implementation of a new SEPICbased single-switch buck–boost DC–DC converter with continuous input current', IEEE Trans. Power Electron., 2018, 33, (12), pp. 10317–10325

[19] Singh, A.K., Pathak, M.K.: 'Single-stage ZETA-SEPIC-based multifunctional integrated converter for plug-in electric vehicles', IET Electr. Syste. Transp., 2018, 8, (2), pp. 101–111

[20] Du, Y., Zhou, X., Bai, S., et al.: 'Review of non-isolated bi-directional DCDC converters for plug-in hybrid electric vehicle charge station application at municipal parking decks'. 2010 Twenty-Fifth Annual IEEE Applied Power Electronics Conf. Exposition, Palm Springs, CA, USA., 2010, pp. 1145–1151

[21] Kwon, M., Oh, S., Choi, S.: 'High gain soft-switching bidirectional DC–DC converter for eco-friendly vehicles', IEEE Trans. Power Electron., 2014, 29, pp. 1659–1666

[22] Mirzaei, A., Jusoh, A., Salam, Z., et al.: 'Analysis and design of a high efficiency bidirectional DC–DC converter for battery and ultracapacitor applications', Simul. Model. Pract. Theory, 2011, 19, pp. 1651–1667

[23] Han, J.T., Lim, C.-S., Cho, J.-H., et al.: 'A high efficiency non-isolated bidirectional DC-DC converter with zero-voltage-transition'. 2013 - 39th Annual Conf. IEEE Industrial Electronics Society, 2013, pp. 198–203

[24] Zhang, J., Lai, J.-S., Kim, R.-Y., et al.: 'High-power density design of a softswitching high-power bidirectional DC–DC converter', IEEE Trans. Power Electron., 2007, 22, pp. 1145–1153

[25] Paul, A., Subramanian, K., Sujitha, N.: 'PV-based off-board electric vehicle battery charger using BIDC', Turk. J. Electr. Eng. Comput. Sci., 2019, 27, (4), pp. 2850–2865

[26] Sree, L., Umamaheswari, M.G.: 'A Hankel matrix reduced order SEPIC model for simplified voltage control optimization and MPPT', Sol. Energy, 2018, 170, pp. 280–292

[27] Zhang, J.: 'Bidirectional DC-DC power converter design optimization, modeling and control'. Dissertation, the faculty of the Virginia Polytechnic Institute and State University, Virginia Polytechnic Institute and State University, 2008

[28] Gounden, N.G.A., Krithiga, S.: 'Power electronic configuration for the operation of PV system in combined grid-connected and stand-alone modes', IET Power Electron., 2014, 7, pp. 640–647

[29] Arul Daniel, S., Ammasai Gounden, N.: 'A novel hybrid isolated generating system based on PV fed inverter assisted wind driven induction generators', IEEE Trans. Energy Convers., 2004, 19, (2), pp. 416–422